ORIGINAL RESEARCH

Computational fluid dynamics of upper airway aerodynamics for exercise-induced laryngeal obstruction: A feasibility study

Michael Döllinger PhD [1] | Bernhard Jakubaß PhD [1] | Hu Cheng PhD [2] |
Stephen J. Carter PhD [3] | Stefan Kniesburges PhD [1] 🔘 | Bea Aidoo BS [4] |
Chi Hwan Lee PhD [5] | Claudio Milstein PhD [6] | Rita R. Patel PhD [7] 🔘

[1]Division of Phoniatrics and Pediatric Audiology at the Department of Otorhinolaryngology Head & Neck Surgery, University Hospital Erlangen, Friedrich-Alexander-Universität Erlangen-Nürnberg, Erlangen, Germany

[2]Department of Psychological and Brain Sciences, Program of Neuroscience, Indiana University, Bloomington, Indiana, USA

[3]Department of Kinesiology, School of Public Health, Indiana University, Bloomington, Indiana, USA

[4]Department of Medicine, Indiana University School of Medicine, Bloomington, Indiana, USA

[5]Department of Biomedical Engineering & Mechanical Engineering, Purdue University, West Lafayette, Indiana, USA

[6]Department of Otolaryngology-Head & Neck Surgery, Cleveland Clinic Lerner and Case Western Reserve University Schools of Medicine, Head and Neck Institute, Cleveland Clinic, Cleveland, Ohio, USA

[7]Department of Speech, Language, and Hearing Sciences and Department of Otolaryngology Head and Neck Surgery, Indiana University, Bloomington/Indianapolis, Indiana, USA

Correspondence
Rita R. Patel, CCC-SLP, Department of Speech, Language, and Hearing Sciences and Department of Otolaryngology Head and Neck Surgery, Indiana University School of Medicine, 1130 W. Michigan St., Fesler Hall, Suite 400, Indianapolis, IN 46202, USA.
Email: patelrir@iu.edu

Abstract

Objective: Use of computational fluid dynamic (CFD) simulations to measure the changes in upper airway geometry and aerodynamics during (a) an episode of Exercise-Induced Laryngeal Obstruction (EILO) and (b) speech therapy exercises commonly employed for patients with EILO.

Methods: Magnetic resonance imaging stills of the upper airway including the nasal and oral cavities from an adult female were used to re-construct three-dimensional geometries of the upper airway. The CFD simulations were used to compute the maximum volume flow rate (l/s), pressure (Pa), airflow velocity (m/s) and area of cross-section opening in eight planes along the vocal tract, separately for inhalation and exhalation.

Results: Numerical predictions from three-dimensional geometrical modeling of the upper airway suggest that the technique of nose breathing for inhalation and pursed lip breathing for exhalation show most promising pressure conditions and cross-sectional diameters for rescue breathing exercises. Also, if EILO is due to the constriction at the vocal fold level, then a quick sniff may also be a proper rescue inhalation exercise. EILO affects both the inspiratory and the expiratory phases of breathing.

Conclusions: A prior knowledge of the supraglottal aerodynamics and the corresponding upper airway geometry from CFD analysis has the potential to assist the clinician in choosing the most effective rescue breathing technique for optimal functional outcome of speech therapy intervention in patients with EILO and in understanding the pathophysiology of EILO on a case-by-case basis with future studies.

Level of Evidence: 4

KEYWORDS
computational fluid dynamics (CFD), exercise-induced laryngeal obstruction (EILO), paradoxical vocal fold motion, speech therapy, voice therapy

1 | INTRODUCTION

Exercise-induced laryngeal obstruction (EILO) also called vocal cord dysfunction/paradoxical vocal fold motion, is a term that is now being used to describe a condition where there is episodic reversible narrowing of the laryngeal/supralaryngeal structures during exercise.[1] EILO has been reported to predominantly affect the inspiratory phase of the breathing cycle; however, the exact pathophysiological mechanisms responsible for EILO are unknown.[2]

Management of EILO requires a multidisciplinary approach involving direct exercises to maintain an open airway.[3-6] Behavioral intervention provided by speech-language pathologists, targeted toward exercises that result in an adequate upper airway opening during inhalation are the mainstay of treatment in individuals with EILO. A variety of breathing techniques such as quick sniff (QS) nasal breathing,[7] panting,[8] abdominal breathing,[9] pursed-lip breathing,[10] and bi-phasic inspiratory breathing[10] have been reported to achieve an "open throat breathing"/"vocal fold opening" in literature. However, physiological studies quantifying the degree of vocal fold/supraglottic opening and aerodynamic characteristics resulting from the various breathing techniques are lacking.

Computational fluid dynamic (CFD) simulations have been applied to understand the airway anatomy and physiology of airway obstructions resulting from obstructive sleep apnea and subglottal stenosis[11-13]; to simulate surgical conditions of airway,[14-16] to evaluate and treat upper airway collapse during exercise in race horses[17-19]; and to simulate vocal fold adduction digitally and evaluate changes in inspiratory flow.[20] To the best of our knowledge, similar techniques have not been applied to the selection of management strategies for EILO or to investigate the pathophysiology of an actual EILO event.

Studies utilizing CFD simulations in airway research have concentrated either on evaluating only inhalation,[21-23] exhalation,[24] or investigating phonation as a special case of exhalation.[25,26] Though useful, these do not provide a realistic picture of breathing which is a continuous cycle. Furthermore, several CFD simulations have concentrated on the airway up to the nasopharynx,[12,23] neglecting the entire nasal and oral cavities, or even completely focused on the bronchial bifurcation region[27] and region from the lower mandibular plane.[24] Some studies have also transformed the geometry of the airway into an artificial straight row of cylinders with realistic diameters,[25,28] while other studies used the actual airway geometry.[11,12,23,24,27] In this study, we utilize the entire upper airway geometry including both the nostrils and mouth up to the subglottal level below the vocal folds to simulate the aerodynamic characteristics during breathing exercises and an EILO event.

During typical breathing, the relationship between the upper airway geometry and airflow/pressure during inhalation and exhalation is predictable. Based on the Bernoulli principle, in EILO it has been proposed that a narrow cross-section area of the laryngeal/supralaryngeal structures results in greater air velocity compared to the tube of a greater diameter. This, in turn, results in negative relative pressures in the constriction and a greater risk of airway collapsing,

which creates temporary obstruction.[29] It has been postulated that the breathing exercises for EILO should attenuate the "early high velocity" stage of inspiration to prevent increased airflow and collapse of structures in the laryngeal inlet.[2] However, the relationship between the upper airway geometry and airflow/pressure during inhalation and exhalation in EILO during various exercises has not been explored. The aim of this preliminary study is to use a CFD model of the human upper airway to:

1. Evaluate the relationship between area, volume flow rate, and pressures during rest breathing, panting, pursed lip breathing, QS, and deep nose breathing to address the question: which breathing exercise results in greater opening at the vocal folds and supraglottal areas without causing excessive volume flow rate and pressures?
2. Evaluate the relationship between area, volume flow rate, and pressures during EILO with stridor.

2 | MATERIALS AND METHODS

2.1 | Data collection

A 47-year-old vocally healthy female underwent magnetic resonance imaging (MRI) of the vocal tract. The MRI was obtained for the following six experimental tasks: rest breathing (nose only), deep mouth breathing/panting (mouth only), pursed lip breathing (PLB) (mouth only), EILO with stridor on inhalation (mouth only), QS (nose only), and deep nose breathing (nose only).

The MRI scan was performed on a Siemens 3T Prisma scanner with a 64-channel head coil at the Imaging Research Facility of Indiana University, Bloomington. A Turbo spin-echo pulse sequence with BLADE trajectory and restore pulse was used to achieve high resolution and short scan time while mitigating motion artifacts. The acquisition parameters were: Field of view $= 320$ mm; TR/TE $= 5500/109$ ms; Matrix $= 320 \times 320$; Number of slices $= 50$; Slice thickness $= 2$ mm; Flip angle $= 90°$; Bandwidth $= 363$ Hz/pixel; Turbo factor $= 28$; Grappa acceleration factor $= 2$; Concatenation $= 2$. The image resolution is $1 \times 1 \times 2$ mm^3. The total scan time was 2:03 min for each task.

The time-varying airflow rate (mL/s) from the Phonatory Aerodynamic System (6600 PENTAX Medical, Montvale, NJ) was used as the input flow for the CFD simulations. The study was conducted as per Indiana University Institutional Review Board requirements of informed consent.

2.2 | Numerical simulation

Numerical methods: The flow simulations were carried out with the CFD software STAR-CCM+ (Version 2020.2, Siemens PLM Software, Plano, TX, USA) assuming incompressible flow conditions. The turbulence flow was simulated based on the unsteady Reynolds-averaged

Navier–Stokes equations in combination with the SST (shear stress transport) k–ω model. The pressure-correction pressure-implicit with splitting operators algorithm was used to solve the pressure–velocity linked equations non iteratively. An algebraic multigrid method with a Gauss–Seidel relaxation scheme was applied to solve the final linear system of equations.

Geometry: The vocal tract geometries were segmented from the MRI scans with 3D Slicer version 4.10.1.[30] For tasks with closed mouth (e.g., nose breathing, QS, and deep nose breathing), the oral cavity was not segmented, as the transition coming from the supraglottal region was mostly blocked by the tongue. The segmented geometries of the vocal tracts were imported into STAR-CCM+ and a polyhedral volume mesh with a base size of 0.5 mm was created, resulting in grids with 0.7–0.9 million cells, depending on the presence of the oral cavity.

Boundary conditions: The vocal tract walls were defined as solid walls with no-slip conditions. The opening toward the lung was defined as a mass flow inlet (as the lung physiologically drives the flow in the vocal tract) while the mouth opening, if present, and the nostrils were defined as pressure outlets. In the cases of mouth-only breathing, the nostrils were also defined as solid walls. The dynamic viscosity of air was specified as $v = 1.8551 \times 10^{-5}$ m^2/s and the density of air constant at $\rho = 1.18415$ kg/m^3 as the Mach number is Ma <0.3.[31] The time step was set to 10^{-5} s. For the input flow from the lungs, the actual transient flow measured from the Phonatory Aerodynamic System (6600 PENTAX Medical, Montvale, NJ) for the experimental conditions over six full breathing cycles (inhalation and exhalation) was utilized. The signal was low-pass filtered with a butterworth filter of second order and a cut-off frequency of 200 Hz to produce a smooth input signal for the simulation. At the beginning of the simulation, the flow was kept constant for 0.3 s to initialize the flow field.[26]

Computed parameters: The volume flow rate (l/s), pressure (Pa), and velocity magnitude (m/s) were measured along the flow direction in the nasopharyngeal, oropharyngeal, supraglottal, epiglottis, glottal,

and subglottal planes, as well as in the nostrils (separately for left and right nostrils) and mouth opening (Figure 1). The demarcation of the various planes in the computed geometry was done in consultation with a laryngologist from the Indiana University Health Voice Center. Each of the six cycles was partitioned into an inhalation and exhalation phase at the zero crossing of the flow. The parameters were computed as follows: In each cycle for each time step, the mean values were computed over each plane. The resulting inhalation/exhalation curves were averaged over the six cycles. From there the maximal absolute values, and mean cycle values (including standard deviations) were taken for inhalation and exhalation. Plane areas (mm^2) were computed based on the MRI images.
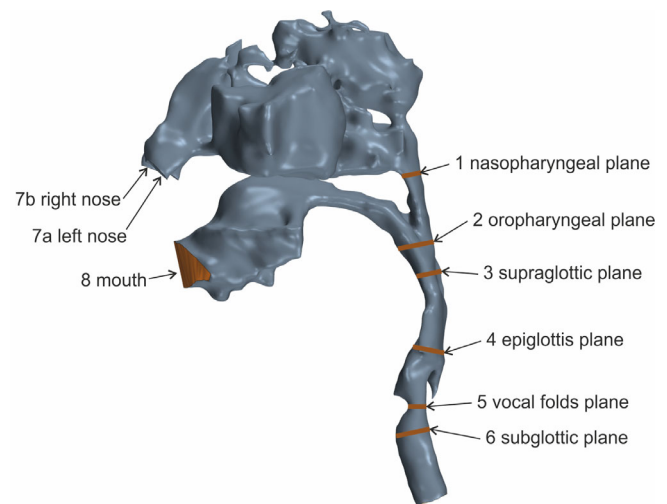
FIGURE 1 Reconstructed three-dimensional geometry of the upper airway depicting the planes where parameters were computed.
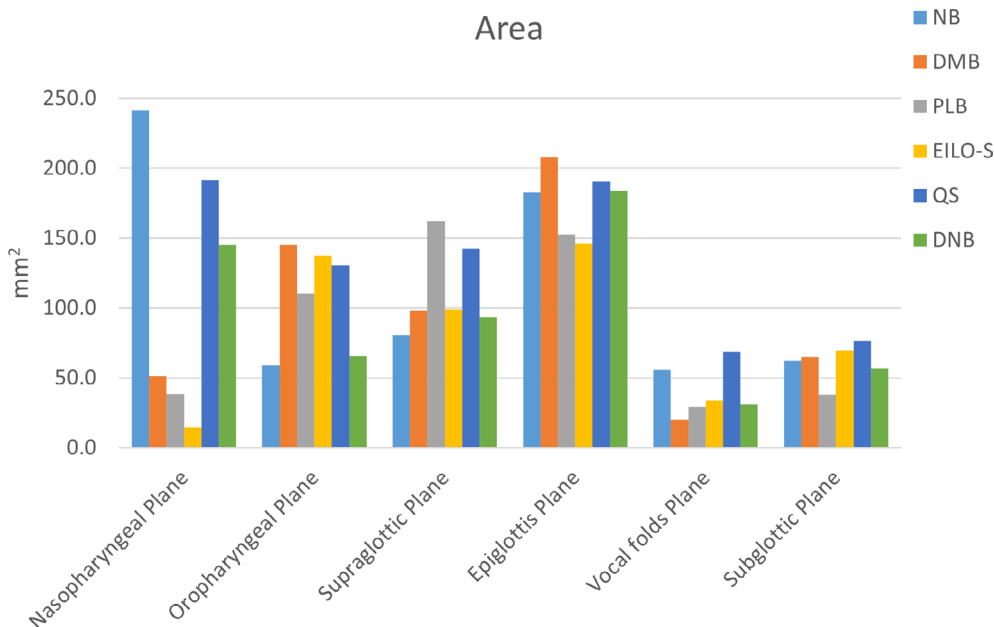
FIGURE 2 Area (mm^2) across the six different anatomical planes for the six experimental conditions: tasks: nose breathing (NB), deep mouth breathing (DMB), pursed lip breathing (PLB), simulated exercise-induced laryngeal obstruction with stridor (EILO-S), quick sniff (QS), and deep nose breathing (DNB).

TABLE 1 Maximum volume airflow rate (L/s) during inhalation and exhalation across the eight different anatomical planes for the six experimental tasks: nose breathing (NB), deep mouth breathing (DMB), pursed lip breathing (PLB), simulated exercise-induced laryngeal obstruction with stridor (EILO-S), quick sniff (QS), and deep nose breathing (DNB).

Maximum volume flow values [L/s] for inhalation

	NB	DMB	PLB	EILO-S	QS	DNB
Nose right + left	−0.162	na	na	na	−0.844	−1.418
Mouth	na	−1.856	−0.593	−0.507	na	na
Nasopharyngeal	−0.162	0.000	0.000	0.000	−0.842	−1.416
Oropharyngeal	−0.162	−1.855	−0.591	−0.508	−0.844	−1.417
Supraglottic	−0.162	−1.854	−0.592	−0.506	−0.844	−1.417
Epiglottis	−0.162	−1.852	−0.592	−0.505	−0.843	−1.415
Vocal folds	−0.162	−1.842	−0.589	−0.506	−0.842	−1.413
Subglottic	−0.162	−1.856	−0.592	−0.509	−0.843	−1.416

Maximum volume flow values [L/s] for exhalation

	NB	DMB	PLB	EILO-S	QS	DNB
Nose right + left	1.537	na	na	na	0.231	0.655
Mouth	na	2.470	1.008	0.719	na	na
Nasopharyngeal	0.157	0.009	0.001	0.000	0.230	0.650
Oropharyngeal	0.156	2.463	1.007	0.722	0.230	0.649
Supraglottic	0.157	2.465	1.007	0.718	0.230	0.649
Epiglottis	0.157	2.463	1.007	0.717	0.230	0.654
Vocal folds	0.156	2.447	1.004	0.718	0.230	0.648
Subglottic	0.156	2.462	1.005	0.719	0.230	0.649

Note: "na" means that no value was computed due to experimental condition.

TABLE 2 Maximum pressure (Pa) during inhalation (negative pressure) and exhalation across the eight different anatomical planes for the six experimental conditions: tasks: nose breathing (NB), deep mouth breathing (DMB), pursed lip breathing (PLB), simulated exercise-induced laryngeal obstruction with stridor (EILO-S), quick sniff (QS), and deep nose breathing (DNB).

Maximum pressure values [Pa] for inhalation

	NB	DMB	PLB	EILO-S	QS	DNB
Nose right	−1.2	na	na	na	−274.5	−73.4
Nose left	−13.1	na	na	na	−475.4	−239.3
Mouth	na	−9.0	−286.1	−1.2	na	na
Nasopharyngeal	−13.1	−225.2	−449.6	−40.7	−414.2	−571.2
Oropharyngeal	−20.0	−231.0	−449.3	−42.6	−440.8	−880.7
Supraglottic	−19.5	−312.9	−364.1	−37.7	−436.5	−805.4
Epiglottis	−23.3	−463.6	−451.6	−72.5	−461.1	−929.5
Vocal folds	−27.4	−5414.8	−705.0	−274.3	−543.8	−2099.4
Subglottic	−28.2	−5387.7	−688.4	−257.5	−531.7	−2226.4

Maximum pressure values [Pa] for exhalation

	NB	DMB	PLB	EILO-S	QS	DNB
Nose right	0.0	na	na	na	0.0	0.0
Nose left	0.0	na	na	na	0.0	0.0
Mouth	na	0.0	0.0	0.0	na	na
Nasopharyngeal	19.8	676.5	1770.1	151.1	50.9	131.5
Oropharyngeal	20.0	216.1	1611.5	58.6	51.8	144.2
Supraglottic	21.7	25.2	1362.2	52.8	52.1	162.1
Epiglottis	26.8	9.3	1617.9	65.8	53.1	141.9
Vocal folds	27.0	11.7	1522.7	216.3	52.6	161.0
Subglottic	28.9	5422.9	1820.9	489.1	54.3	386.8

Note: "na" means that no value was computed due to experimental condition.

3 | RESULTS

3.1 | Area (mm²)

Figure 2 shows the area (mm²) across the eight different planes for the six experimental conditions: nose breathing (NB), deep mouth breathing (DMB), PLB, QS, DNB, and EILO-S. For the nasopharyngeal plane, the area is greater for NB. Overall, the vocal fold plane shows smallest areas followed by the subglottal plane, across all tasks. For the task of NB and QS, the glottal area is not as narrow as in the other paradigms with the area being more than 50 mm² (Figure 2). The task of QS has the largest area at the vocal fold compared to any other experimental task.

3.2 | Volume flow rate (l/s)

As expected, the volume flow for inhalation is negative due to the opposite flow direction, compared to exhalation. Based on volume flow, the experimental tasks can be divided into two groups: maximum volume flow <1 L/s (NB < EILO-S < PLB < QS) and >1 L/s

(DNB < DMB) (Table 1). During inhalation, the maximum volume flow is constant across all involved planes within each task. Anatomic areas that were not involved in the experimental paradigm, like the nasopharyngeal plane in EILO-S correctly show no airflow volume. The range of maximum volume flow vary considerably between tasks; for example, DMB achieved 11 times more volume flow than NB.

For exhalation, the experimental tasks can be divided into two groups with maximum flow volume of <1 L/s (NB < QS < DNB < EILO-S) and >1 L/s (PLB < DMB). Similar to inhalation, these flow relations for exhalation also have constant maximum values across all nine planes within each task. The range of maximum volume flow also vary considerably between tasks, whereas DMB again achieves 11 times more maximum volume flow than NB.

3.3 | Pressure (Pa)

As expected, the relative pressure values for inhalation are negative (Table 2). Overall, within each task, highest pressure values were
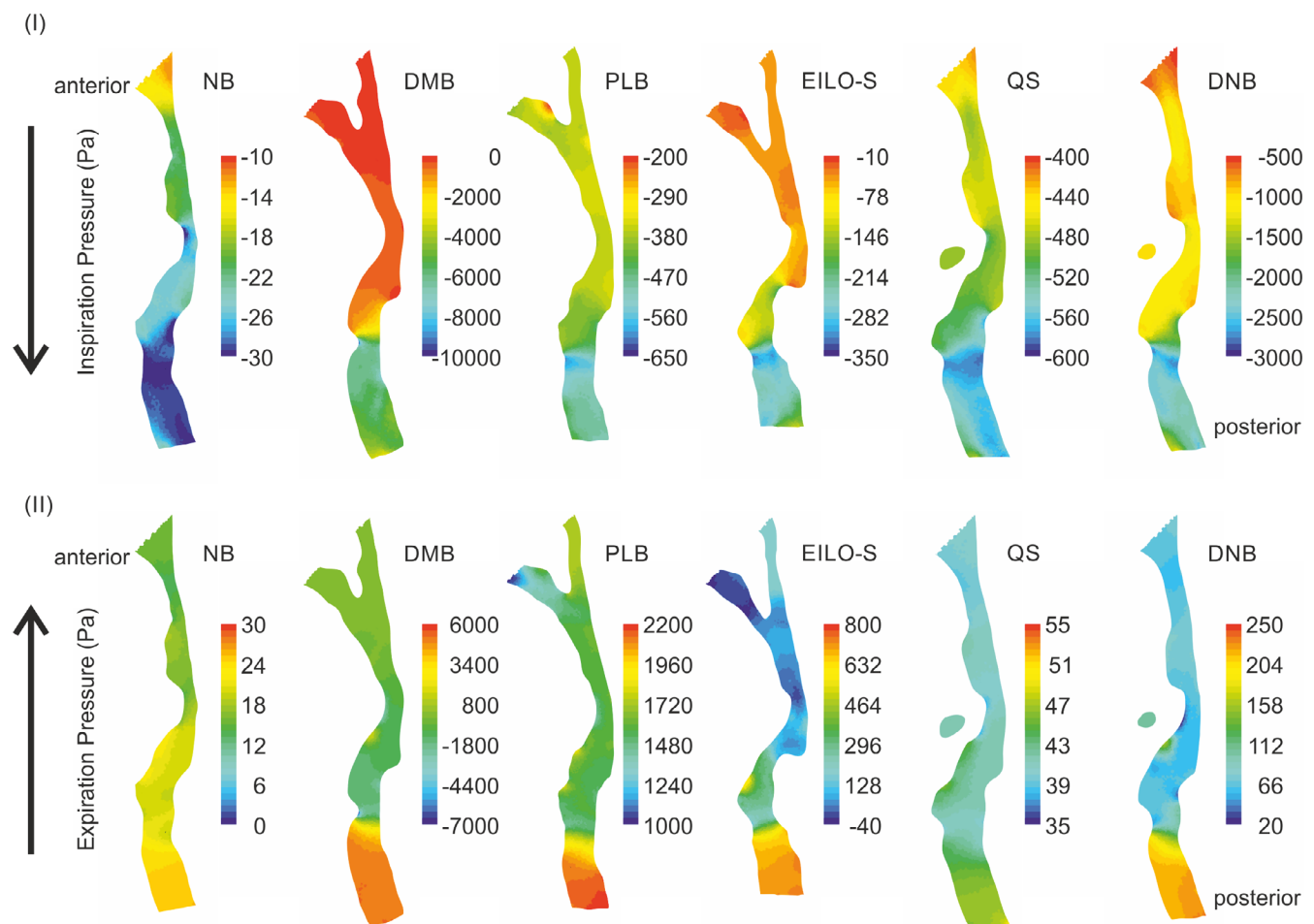
FIGURE 3 Pressure in midsagittal plane during inspiration (I) and expiration (II) at time-step for maximum inhalation/exhalation flow for the six experimental tasks: nose breathing (NB), deep mouth breathing (DMB), pursed lip breathing (PLB), simulated exercise-induced laryngeal obstruction with stridor (EILO-S), quick sniff (QS), and deep nose breathing (DNB).

TABLE 3 Maximum airflow velocity (m/s) during inhalation and exhalation across the eight different anatomical planes for the six experimental conditions: tasks: nose breathing (NB), deep mouth breathing (DMB), pursed lip breathing (PLB), simulated exercise-induced laryngeal obstruction with stridor (EILO-S), quick sniff (QS), and deep nose breathing (DNB).

Maximum flow velocities [m/s] for inhalation						
	NB	DMB	PLB	EILO-S	QS	DNB
Nose right	1.41	na	na	na	21.39	10.82
Nose left	4.65	na	na	na	28.16	18.83
Mouth	na	3.74	21.63	0.19	na	na
Nasopharyngeal	1.15	0.81	0.51	0.00	5.21	12.57
Oropharyngeal	2.65	14.13	6.74	4.72	6.42	21.63
Supraglottic	2.01	18.46	4.59	5.05	5.87	15.73
Epiglottis	1.10	15.67	5.39	7.38	6.10	10.58
Vocal folds	2.90	89.68	19.66	16.54	12.22	45.69
Subglottic	2.61	35.04	15.80	9.54	10.79	28.86
Maximum flow velocities [m/s] for exhalation						
	NB	DMB	PLB	EILO-S	QS	DNB
Nose right	2.02	na	na	na	7.12	6.36
Nose left	4.47	na	na	na	7.86	10.60
Mouth	na	8.27	38.80	0.52	na	na
Nasopharyngeal	0.90	7.77	2.42	0.14	1.31	6.29
Oropharyngeal	2.57	22.94	13.41	7.93	1.72	9.75
Supraglottic	1.92	28.94	8.62	7.50	1.58	7.76
Epiglottis	1.23	23.29	10.68	9.53	1.59	7.44
Vocal folds	2.76	118.38	33.37	22.26	3.29	20.85
Subglottic	2.39	37.68	26.05	10.03	2.88	11.32

Note: "na" means that no value was computed due to experimental condition.

consistently observed at the vocal fold plane during inhalation and at the subglottic plane during exhalation (Figure 3); where the smallest diameters for the volume flow rate are present. For inhalation, DMB shows highest negative pressure followed by DNB > PLB > QS > EILO-S at the level of the vocal folds. NB shows the smallest pressure values (< 30 Pa) across all anatomical planes. Pressure values show a high range between tasks, with negative pressures for DMB being almost 200 times higher than for NB.

For exhalation, at the subglottic plane, DMB shows again the largest values, followed by PLB > EILO-S > DNB > QS > NB. At the laryngeal and the various supraglottal planes, the pressure values were consistently higher for PLB compared to QS.

For DMB, the highest negative pressure is detected, followed by DNB. Hence, for these two paradigms, the largest pressure forces act on the airway boundaries.
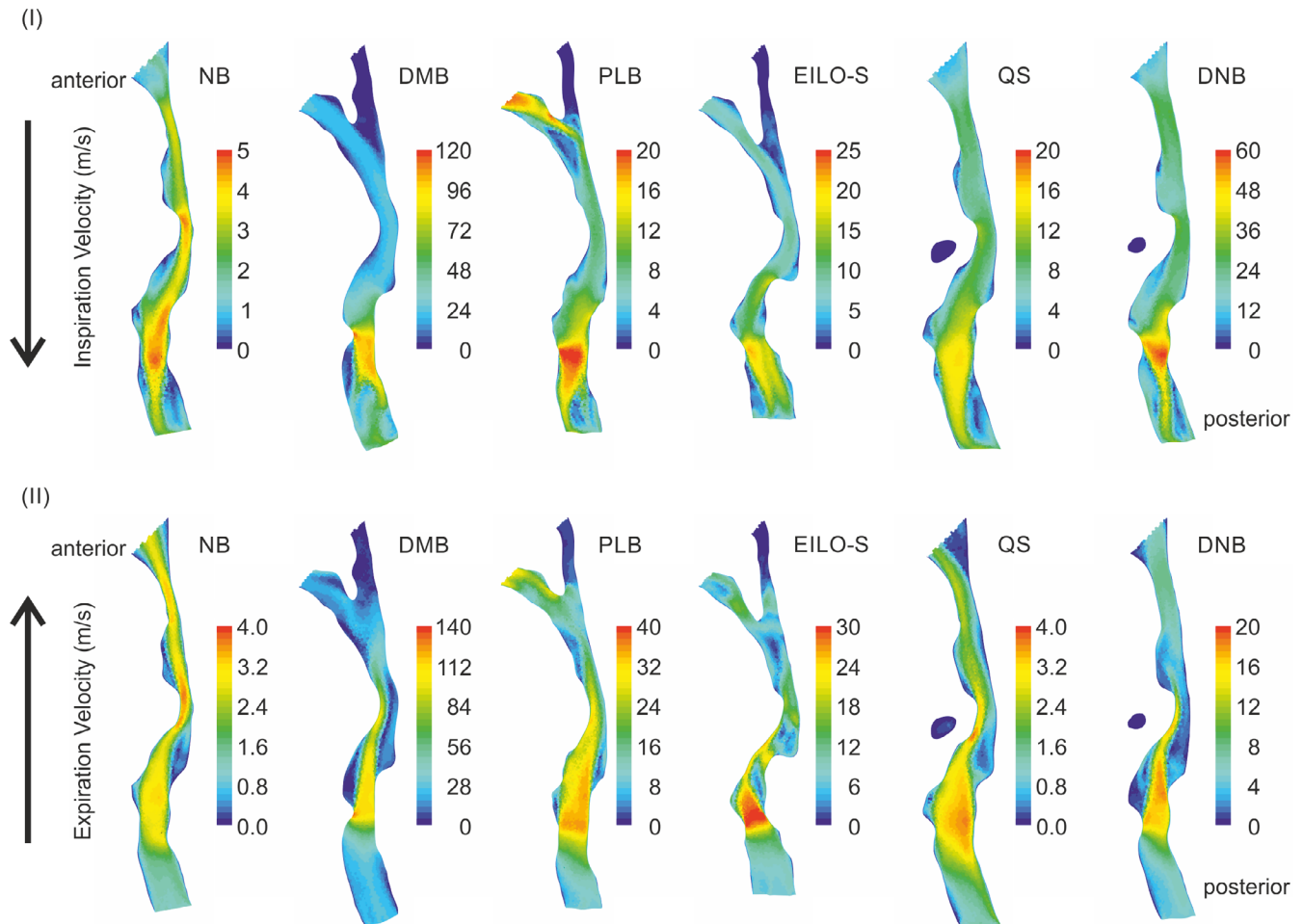
3.4 | Velocity (m/s)

For both inhalation and exhalation, within each paradigm, the velocity is always highest at the vocal fold plane where the smallest diameter of the cross-section occurs (Table 3, Figure 4). During inhalation, velocities for DMB are up to 31 times larger than for NB and for exhalation even 43 times larger at the vocal fold plane. DMB shows by far the highest velocities during inhalation and exhalation compared to all the experimental tasks. The maximum velocity values are mainly around the glottic plane (Table 3), except for NB, where also at the oropharyngeal plane high values occur.

4 | DISCUSSION

EILO is the current consensus term that is used for conditions also known as paradoxical vocal fold motion or vocal cord dysfunction,[32] due to primary collapse of either the glottal or supraglottal structures in the airway in response to exercise as a trigger.[33,34] EILO is well-recognized as a distinct entity and a sub-type under the broader term of inducible laryngeal obstruction (ILO), which represents a subset of patients with ILO who only develop symptoms of shortness of breath with exercise,[35] and the other sub-category being irritant induced laryngeal obstruction, where the triggers involve irritants such as

FIGURE 4 Velocity (m/s) in midsagittal plane during inspiration (I) and expiration (II) for the six experimental tasks: nose breathing (NB), deep mouth breathing (DMB), pursed lip breathing (PLB), simulated exercise-induced laryngeal obstruction with stridor (EILO-S), quick sniff (QS), and deep nose breathing (DNB). The glottal jet above (expiration) and below (inspiration) the vocal folds are also visible.
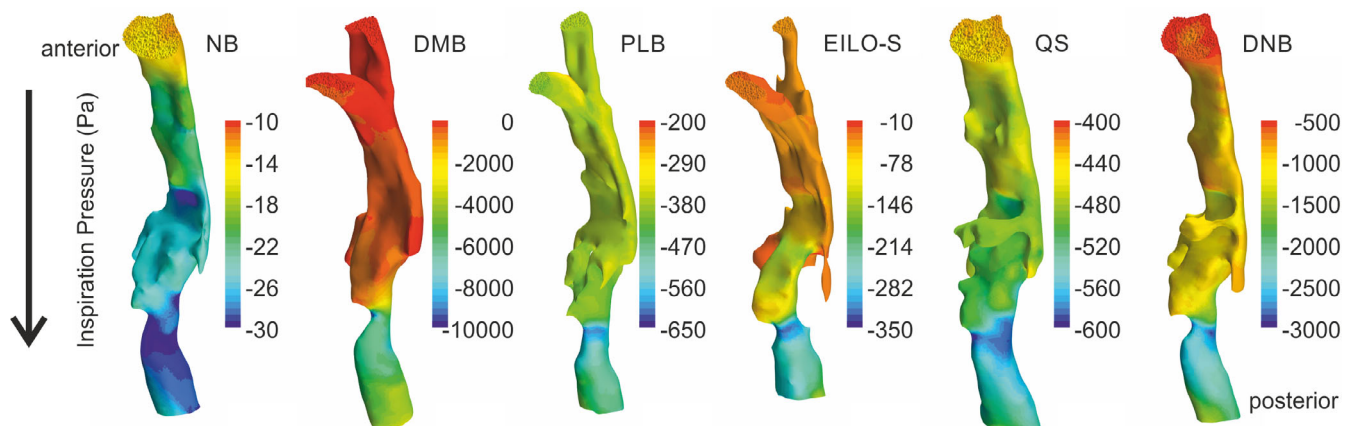
FIGURE 5 The 3D view of upper airway. The pressure on the walls of the upper airway during inspiration for the six experimental tasks: nose breathing (NB), deep mouth breathing (DMB), pursed lip breathing (PLB), simulated exercise-induced laryngeal obstruction with stridor (EILO-S), quick sniff (QS), and deep nose breathing (DNB).

smoke, gas, airborne pollutants, odors, reflux, and so forth.[32] In the current work, CFD analysis provides important insights into the: (a) impact of the speech therapy exercises and (b) EILO obstruction on upper airway area and aerodynamics. Another innovative aspect of this study is that it considers the continuous flow for inhalation/exhalation and real flow data instead of artificial volume flow rate.

4.1 | Which breathing exercise results in greater opening at the vocal folds and supraglottal areas without causing excessive airflow and pressures?

For EILO therapy, exercises may be desired that result in an adequate upper airway opening during inhalation (Figure 2). Furthermore, low negative or even positive pressure during inhalation may be desired to avoid collapsing of tissue based on too high relative negative pressure in the airway (Figure 3, Table 2) and toward the airway walls (Figure 5). Based on the aerodynamic principle of Bernoulli effect the narrow the area of the laryngeal/supralaryngeal structures the greater the air velocity is which in turn results in negative relative pressures at the location of constriction increasing the risk of an airway collapse and obstruction.[29]

Additionally, during exhalation, one might want an exercise that helps to open the upper airways. This can be achieved by exercises producing relatively high air pressure during exhalation for a large continuous region (i.e., avoiding the Bernoulli effect) within the upper airways. Based on these assumptions the following can be stated from the findings of this study.

For inhalation, deep mouth breathing seems to be the worst exercise, since it shows the smallest glottal area along with the highest air volume (Table 1) resulting in highest airflow velocities (Table 3, Figure 4) and hence largest relative negative pressure in the airway (Table 2, Figure 3) and on the airway tissue (Figure 5). Nose breathing seems to be the best inhalation exercise due to little negative pressures and large glottal opening. The other four exercises show worse pressure conditions in the upper airways than EILO-S (Table 2) although QS exhibits a larger glottal area than EILO-S (Figure 1). Thus, it appears that if the EILO is due to the constriction at the vocal fold level, then a QS may also be a proper rescue inhalation exercise. One might expect the glottal area for EILO-S to be almost negligible, if not the smallest possible. However, in this single participant, although the glottal area for EILO-S was indeed small, it did not approach zero. Future studies with a large number of participants are needed, to comprehensively explore the impact of the respiratory cycle and the glottal area. Additionally, utilizing MRI with retrospective gating,[36] would enable the recording of inhalation and exhalation in real-time during the MRI scan, providing a more comprehensive understanding.

For exhalation, PLB seems to be the best exercise, since overall continuous high air pressure values occur, due to similar large areas of oropharyngeal, supraglottic and epiglottic planes (Figure 2), keeping the upper airways open. Other potential exercises may be QS; nose breathing (large glottal area but small pressure values) and deep nose breathing (high pressure values but small glottal area). Again, deep mouth breathing seems to be the worst exercise due to small glottal area, small pressures at vocal folds, epiglottis and supraglottic planes, although deep mouth breathing exhibits highest subglottal pressure values.

It has been demonstrated that EILO could also occur due to constriction predominantly at the level of the supraglottics.[33,34] For predominantly supraglottal obstruction resulting in EILO, the findings of this study suggest that besides PLB during exhalation, also inhalation exercise of QS may be effective due to rather continuous and large airway area cross sections.

4.2 | Relationship between area, airflow, and pressures during EILO with stridor (EILO-S)

Compared to normal breathing behavior EILO-S exhibits much higher volume flows during inhalation (Table 1). This larger inhalation flow and smaller cross-sectional areas (Figure 2) yield higher flow velocities (Table 3) and also considerably more negative pressure during inhalation (Table 2) yielding a higher risk of tissue collapsing.

For exhalation, volume flow, air velocity and especially pressure values are increased for EILO-S. The considerable increase in pressure, especially at the subglottic and vocal folds planes, indicates a substantially higher effort for exhalation compared to normal breathing.

Overall, the flow volume–pressure relationship (Table 1, Table 2) at the vocal fold and subglottic planes for EILO-S are much worse than for normal breathing, that is, there is more pressure for the same amount of volume flow rate in EILO-S. This confirms findings from Frank-Ito et al.[20] where they simulated a vocal fold adduction digitally to mimic EILO rather than a person reproducing an episode in this study.[20] Prior studies using animal models have demonstrated a substantial increase in upper tracheal/subglottal pressures to be linked to hypocapnia/arterial partial pressure of carbon dioxide (reduced $PaCO_2$) and increased laryngeal closure reflex.[37,38] The relationship between reflexive glottal closure and hypocapnia needs to be further investigated in patients with EILO in future studies. Stridor/noisy breathing is one of the three most common symptoms (the other two being shortness of breathy and throat tightness) of patients with EILO.[4,39–41] Not all patients with EILO may present with stridor. Future studies should empirically evaluate changes in upper airway geometry and aerodynamics in patients' EILO with and without noisy breathing.

5 | CONCLUSIONS

This numerical study revealed advantages and disadvantages of potential speech therapy exercises for EILO and the aerodynamic characteristics of EILO with stridor. The best rescue exercise appears to be nose breathing or QS for inhalation and PLB for exhalation. This numerical study already showed several advantages in investigating volume flow rate characteristics applying CFD in an EILO attack that cannot be measured or visualized otherwise. Patient-specific volume flow rate characteristics can be obtained based on CT/MRI scans in absence of the patients. However, only one healthy subject was investigated in this study and hence the findings from actual patients may be different. Furthermore, simulated EILO-S may not reflect what happens during unsimulated attack. We plan to recruit patients with

EILO and use their input flow from exercise for a closer approximation to reality on an actual EILO attack. Using CFD analysis to select the most optimal strategy to establish upper airway airflow and understand the pathophysiology of EILO has the potential to greatly reduce the impact of the disorder and improve functional outcomes in patients with EILO.

CONFLICT OF INTEREST STATEMENT

The authors declare no conflicts of interest.

ORCID

Stefan Kniesburges https://orcid.org/0000-0002-4902-0534
Rita R. Patel https://orcid.org/0000-0002-5354-5210

REFERENCES

1. Halvorsen T, Walsted ES, Bucca C, et al. Inducible laryngeal obstruction: an official joint European Respiratory Society and European laryngological society statement. *Eur Respir J*. 2017;50(3):1602221.
2. Hull JH, Godbout K, Boulet LP. Exercise—associated dyspnea and stridor: thinking beyond asthma. *J Allergy Clin Immunol Pract*. 2020;8(7): 2202-2208.
3. Olin JT, Clary MS, Deardorff EH, et al. Inducible laryngeal obstruction during exercise: moving beyond vocal cords with new insights. *Phys Sportsmed*. 2015;43(1):13-21.
4. Patel RR, Venediktov R, Schooling T, Wang B. Evidence-based systematic review: effects of speech-language pathology treatment for individuals with paradoxical vocal fold motion. *Am J Speech Lang Pathol*. 2015;24(3):566-584.
5. Blager FB. Paradoxical vocal fold movement: diagnosis and management. *Curr Opin Otolaryngol Head Neck Surg*. 2000;8:180-183.
6. Sandage MJ, Milstein CF, Nauman E. Inducible laryngeal obstruction differential diagnosis in adolescents and adults: a tutorial. *Am J Speech Lang Pathol*. 2022;16:1-17.
7. Christopher KL, Wood RP 2nd, Eckert RC, Blager FB, Raney RA, Souhrada JF. Vocal-cord dysfunction presenting as asthma. *N Engl J Med*. 1983;308(26):1566-1570.
8. Rameau A, Foltz RS, Wagner K, Zur KB. Multidisciplinary approach to vocal cord dysfunction diagnosis and treatment in one session: a single institutional outcome study. *Int J Pediatr Otorhinolaryngol*. 2012; 76(1):31-35.
9. Newsham KR, Klaben BK, Miller VJ, Saunders JE. Paradoxical vocal-cord dysfunction: management in Athletes. *J Athl Train*. 2002;37(3): 325-328.
10. Johnston KL, Bradford H, Hodges H, Moore CM, Nauman E, Olin JT. The Olin EILOBI breathing techniques: description and initial case series of novel respiratory retraining strategies for athletes with exercise-induced laryngeal obstruction. *J Voice*. 2018;32(6):698-704.
11. Mylavarapu G, Mihaescu M, Fuchs L, Papatziamos G, Gutmark E. Planning human upper airway surgery using computational fluid dynamics. *J Biomech*. 2013;46(12):1979-1986.
12. Mihaescu M, Murugappan S, Gutmark E, Donnelly LF, Khosla S, Kalra M. Computational fluid dynamics analysis of upper airway reconstructed from magnetic resonance imaging data. *Ann Otol Rhinol Laryngol*. 2008;117(4):303-309.
13. Mihaescu M, Murugappan S, Gutmark E, Donnelly LF, Kalra M. Computational modeling of upper airway before and after adenotonsillectomy for obstructive sleep apnea. *Laryngoscope*. 2008;118(2):360-362.
14. Hudson TJ, Ait Oubahou R, Mongeau L, Kost K. Airway resistance and respiratory distress in laryngeal cancer: a computational fluid dynamics study. *Laryngoscope*. 2023. doi:10.1002/lary.30649. Online ahead of print.
15. Rios G, Morrison RJ, Song Y, et al. Computational fluid dynamics analysis of surgical approaches to bilateral vocal fold immobility. *Laryngoscope*. 2020;130(2):E57-E64.
16. Liu J, Shao Y, Li J, et al. New approach to establish a surgical planning in infantile vallecular cyst synchronous with laryngomalacia based on aerodynamic analysis. *Comput Methods Programs Biomed*. 2023;230: 107335.
17. Rakesh V, Rakesh NG, Datta AK, Cheetham J, Pease AP. Development of equine upper airway fluid mechanics model for thoroughbred racehorses. *Equine Vet J*. 2008;40(3):272-279.
18. Rakesh V, Ducharme NG, Cheetham J, Datta AK, Pease AP. Implications of different degrees of arytenoid cartilage abduction on equine upper airway characteristics. *Equine Vet J*. 2008;40(7):629-635.
19. Strand E, Fjordbakk CT, Holcombe SJ, Risberg A, Chalmers HJ. Effect of poll flexion and dynamic laryngeal collapse on tracheal pressure in Norwegian coldblooded trotter racehorses. *Equine Vet J*. 2009;41(1): 59-64.
20. Frank-Ito DO, Schulz K, Vess G, Witsell DL. Changes in aerodynamics during vocal cord dysfunction. *Comput Biol Med*. 2015;57:116-122.
21. Vial L, Perchet D, Fodil R, et al. Airflow modeling of steady inspiration in two realistic proximal airway trees reconstructed from human thoracic tomodensitometric images. *Comput Methods Biomech Biomed Engin*. 2005;8(4):267-277.
22. Zhang Z, Kleinstreuer C, Kim CS. Computational analysis of micronparticle deposition in a human triple bifurcation airway model. *Comput Methods Biomech Biomed Engin*. 2002;5(2):135-147.
23. Mihaescu M, Gutmark E, Murugappan S, Elluru R, Cohen A, Willging JP. Modeling flow in a compromised pediatric airway breathing air and heliox. *Laryngoscope*. 2009;119(1):145-151.
24. Mylavarapu G, Murugappan S, Mihaescu M, Kalra M, Khosla S, Gutmark E. Validation of computational fluid dynamics methodology used for human upper airway flow simulations. *J Biomech*. 2009; 42(10):1553-1559.
25. Falk S, Kniesburges S, Schoder S, et al. 3D-FV-FE aeroacoustic larynx model for investigation of functional based voice disorders. *Front Physiol*. 2021;12:616985.
26. Jakubaß B, Kniesburges S, Maryn Y, Loomans N, Döllinger M. Simulation der Vokaltraktdurchströmung bei nasaler Phonation. Paper presented at: In Aktuelle phoniatrische-pädaudiologische Aspekte 2019/2020, Band 27. 36. Wissenschaftliche Jahrestagung der DGPP, Göttingen, Germany, 2019. doi:10.3205/19dgpp33"2019
27. Cebral JR, Summers RM. Tracheal and central bronchial aerodynamics using virtual bronchoscopy and computational fluid dynamics. *IEEE Trans Med Imaging*. 2004;23(8):1021-1033.
28. Brouns M, Jayaraju ST, Lacor C, et al. Tracheal stenosis: a flow dynamics study. *J Appl Physiol*. 2007;102(3):1178-1184.
29. Fretheim-Kelly ZL, Halvorsen T, Clemm H, et al. Exercise induced laryngeal obstruction in humans and equines. A Comparative Review. *Front Physiol*. 2019;10:1333.
30. Fedorov A, Beichel R, Kalpathy-Cramer J, et al. 3D slicer as an image computing platform for the quantitative imaging network. *Magn Reson Imaging*. 2012;30(9):1323-1341.
31. Kniesburges S, Thomson SL, Barney A, et al. In vitro experimental investigation of voice production. *Curr Bioinform*. 2011;6(3): 305-322.
32. Christensen PM, Heimdal JH, Christopher KL, et al. ERS/ELS/ACCP 2013 international consensus conference nomenclature on inducible laryngeal obstructions. *Eur Respir Rev*. 2015;24(137):445-450.

33. Roksund OD, Maat RC, Heimdal JH, Olofsson J, Skadberg BT, Halvorsen T. Exercise induced dyspnea in the young. Larynx as the bottleneck of the airways. *Respir Med*. 2009;103(12):1911-1918.

34. Christensen PM, Thomsen SF, Rasmussen N, Backer V. Exercise-induced laryngeal obstructions: prevalence and symptoms in the general public. *Eur Arch Otorhinolaryngol*. 2011;268(9):1313-1319.

35. Chiang T, Marcinow AM, de Silva BW, Ence BN, Lindsey SE, Forrest LA. Exercise-induced paradoxical vocal fold motion disorder: diagnosis and management. *Laryngoscope*. 2013;123(3):727-731.

36. Sheel AW, Foster GE, Romer LM. Exercise and its impact on dyspnea. *Curr Opin Pharmacol*. 2011;11(3):195-203.

37. Nishino T, Yonezawa T, Honda Y. Modification of laryngospasm in response to changes in $PaCO_2$ and PaO_2 in the cat. *Anesthesiology*. 1981;55(3):286-291.

38. Sasaki CT, Suzuki M. Laryngeal spasm: a neurophysiologic redefinition. *Ann Otol Rhinol Laryngol*. 1977;86(2 pt. 1):150-157.

39. Yi JS, Davis AC, Pietsch K, et al. Demographic differences in clinical presentation of pediatric paradoxical vocal fold motion (PVFM). *J Voice*. 2021;S0892-1997((21)):00295.

40. Shay EO, Sayad E, Milstein CF. Exercise-induced laryngeal obstruction (EILO) in children and young adults: from referral to diagnosis. *Laryngoscope*. 2020;130(6):E400-E406.

41. Milstein CF, Patel RR, Laurash E, Kampert M. Identification of breathing pattern disorder in athletes with exercise-induced laryngeal obstruction: a novel assessment tool. *J Voice*. 2023. doi:10.1016/j.jvoice.2023.01.006. Online ahead of print.